Applied Surface Science 257 (2010) 429–433

Contents lists available at ScienceDirect

Applied Surface Science

journal homepage: www.elsevier.com/locate/apsusc

Structural, electrical and mechanical properties of NiO thin films grown by pulsed laser deposition

I. Fasaki [a,b,1], A. Koutoulaki [a,b,1], M. Kompitsas [b,*,1], C. Charitidis [b,1]

[a] National Hellenic Research Foundation, Theoretical and Physical Chemistry Institute, Vasileos Konstantinou Ave. 48, 11635 Athens, Greece
[b] National Technical University of Athens, School of Chemical Engineering, 9 Iroon Polytechniou St., 15780 Zografou, Athens, Greece

ARTICLE INFO

Article history:
Received 26 November 2009
Received in revised form 2 July 2010
Accepted 3 July 2010
Available online 8 July 2010

Keywords:
PLD
Thin film deposition
Nickel oxide
Structural
Electrical
Mechanical properties

ABSTRACT

Nickel oxide (NiO) thin films were prepared by reactive pulsed laser deposition on thermally oxidized Si substrates in 10 Pa oxygen pressure. The substrate temperature during deposition was varied and its influence on the structural, electrical and nanomechanical properties was studied. It was proved that the structural properties were affected by the increase of substrate temperature improving the crystalline structure. Furthermore, a higher substrate temperature resulted in a thicker NiO film, which was attributed to an increased grain size. This effect influenced the electrical properties, too. Resistivity measurements showed that it increased with the increase of substrate temperature. For the first time, the nanomechanical properties of NiO films were studied. The formation and improvement of crystalline structure affected the nanomechanical properties. Nanoindentation testing of NiO thin films revealed an increase of hardness (H) and elastic modulus (E) and a decrease of surface roughness when increasing the substrate temperature.

1. Introduction

NiO is a well-known antiferromagnetic material [1], and a metal-deficient p-type semiconductor [2] with a 3.6 eV band gap [3]. Nickel oxide (NiO) films have a wide range of applications due to their excellent chemical stability. They have been used as catalysts [4], electrochromic display devices [5], fuel cells [6] and gas sensors [7]. NiO thin films usually exhibit p-type conductivity due to holes generated by Ni vacancies in the lattice and therefore NiO is an interesting candidate for materials research. Although structural and electrical properties of NiO films have been studied before, mechanical properties have been less investigated [8].

NiO thin films have been deposited by different techniques, including chemical self-assembling [9], sol–gel [10], RF sputtering [11], DC sputtering [12] and recently pulsed laser deposition (PLD) [13–15]. Preparation methods are essential for determining the microstructure and consequently the functional properties of synthesized structures.

In this work, reactive pulsed laser deposition (RPLD) was used for the deposition of NiO thin films at different substrate temperatures. The effect of substrate heating during deposition on the structural, electrical and nanomechanical properties was studied.

2. Experimental details

The RPLD experiments were performed in a stainless steel vacuum chamber, which was evacuated down to a residual pressure of 6×10^{-4} Pa before the target was irradiated by the laser. Pulses from a KrF* excimer laser ($\lambda = 248$ nm, 10 ns pulse duration) source at 10 Hz repetition rate were focused on the surface of Ni targets. The laser fluence incident on the target surface was set at 5.5 J/cm^2. To deposit each film, 60,000 subsequent laser pulses were applied in 10 Pa oxygen ambient atmosphere.

The target was placed on a pC-controlled XY translator, to avoid drilling under the action of repeated laser pulses. (0 0 1) Si substrates, with a thermally oxidized layer of ca. 190 nm, were placed parallel to the target at a distance of 50 mm. Both targets and substrates were carefully cleaned with acetone in ultrasonic bath before being placed into the vacuum chamber. During film growth the substrates were either kept at room temperature (RT), or heated at constant temperatures 100, 200, 300, 400 °C.

The resistivity of the films was measured using the Van der Pauw method. The crystalline status of the thin films was studied with X-ray diffraction (XRD) using a Philips MRD diffractometer in the $\theta - 2\theta$ mode. The Cu Kα radiation ($\lambda = 1.5418$ Å) was chosen for spectra recording. Optical reflectance measurements were carried

* Corresponding author at: National Hellenic Research Foundation, Theoretical and Physical Chemistry Institute, Greece. Tel.: +30 2107273 834; fax: +30 2107273 794.
E-mail addresses: mcomp@eie.gr, michael.kompitsas@gmail.com (M. Kompitsas).
[1] All authors contributed equally to this work.

0169-4332/$ – see front matter © 2010 Elsevier B.V. All rights reserved.
doi:10.1016/j.apsusc.2010.07.006

out with a PerkinElmer Lambda 19 spectrophotometer within the 300–1000 nm wavelength range.

The indentation analysis was performed using a Hysitron TriboLab® Nanomechanical Test Instrument. The instrument allows the application of loads from 1 to 10,000 μN and the recording of penetration depths as a function of applied loads with a high load resolution (1 nN) and a high displacement resolution (0.04 nm) [16]. A Berkovich diamond indenter was used, with a maximum load range 350–700 μN at room temperature. These loads correspond to a displacement of the indenter into the sample of ~35 nm (<10% of the films' thickness), which is a representative of the film mechanical properties independent of the substrate effect [17].

Experiments were performed in a clean area environment with ~45% humidity and 23 °C ambient temperature. In all depth-sensing tests a total of 10 indents were averaged to determine the mean hardness [*H*] and Young's modulus [*E*] values for statistical purposes, with a spacing of 50 μm. The TriboLab® Nanomechanical Test Instrument employed in this study is equipped with a Scanning Probe Microscope (SPM), in which a sharp probe tip is moved in a raster scan pattern across a sample surface using a three-axis piezo-positioner.

3. Results and discussion

3.1. Structural properties

The X-ray diffractograms of films deposited on Si substrates of different temperatures are shown in Fig. 1. The film deposited at RT is poorly crystallized, the peak centered at 43.3° according to the JCPDS 780643 is attributed to the (2 0 0) lattice plane reflection of the cubic NiO phase. The line seen at 41.9° in this diffractogram could not be definitely assigned: detailed literature research has revealed two candidates for this line. The first one at 41.5° corresponds to the (0 0 2) lattice plane reflection of the metallic Ni cubic phase [18], directly originating from the Ni target. The second one at 42.2° may be due to a Ni_xSi_y compound [19], formed by diffusion in the film–substrate interface. Further research is necessary to clarify this issue.

At higher temperature (100 °C), the intensity of the NiO peak increases and a new peak with low intensity, corresponding to the (2 2 0) lattice plane of NiO, appears. When the substrate temperature is equal to or higher than 200 °C, the main peak at the diffractograms is the (1 1 1).

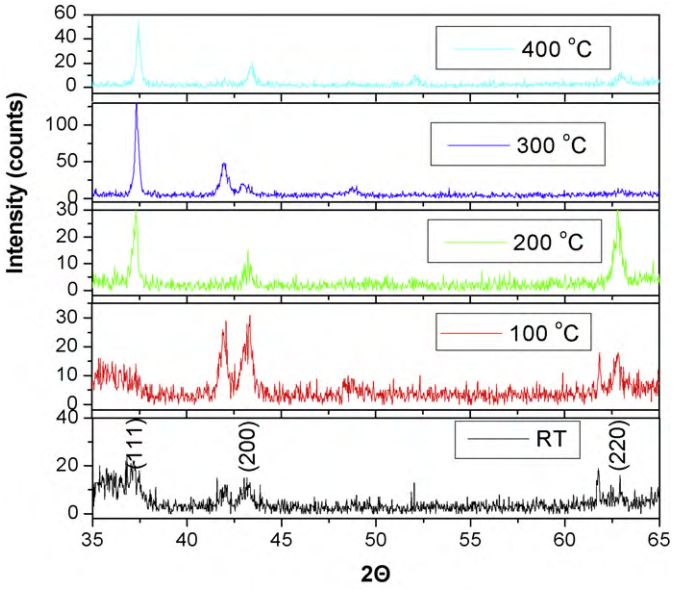

Fig. 1. Diffractograms of films deposited at different temperatures.

Table 1
Grain size as a function of substrate temperature.

Substrate temperature (°C)	Grain size (nm)
RT	19
100	21
200	22
300	21
400	32

NiO films with (2 0 0) or (1 1 1) preferred orientations, are good candidates for the buffer layers of oriented oxide films, such as *c*-axis-oriented perovskite-type ferromagnetic films, and (1 1 1)-oriented spinel-type ferromagnetic films. This is because they are chemically stable, similar in symmetry to the oxygen ion lattice, and their lattice constants are between those of the NiO films and the oriented oxide films. Therefore, NiO film with a preferred crystallographic orientation is important when it is used as a buffer layer. The dependence of crystallinity on substrate temperature can be explained as follows. During the deposition process, atoms travel some distance before they impact on the sample surface to form the deposited film. At higher substrate temperatures, the extra thermal energy provided by the substrate to the atoms is used by the latter to reach equilibrium positions. Therefore, there is greater probability of forming a more perfect crystalline structure at higher substrate temperatures [20].

The average crystallite size *D*, was calculated from the (2 0 0) diffraction line, as it is present in all samples, using the Scherrer formula:

$$D = \frac{0.9 \cdot \lambda}{FWHM \cdot \cos\theta} \quad (1)$$

Here λ = 1.5418 Å, *FWHM* stands for full-width of the diffraction line at half-maximum intensity, while θ is the diffraction angle. As can be seen in Table 1, grain size slightly increases following the heat treatment, which indicates films restructuring, leading to improved crystallinity.

The grain size of nickel oxide grains increases with increasing substrate temperature. At lower substrate temperature, the deposited atoms are expected to have low surface mobility. Restrictive diffusion of atoms prevents crystal growth at energetically favourable sites and promotes atoms to nucleate at new sites. It results in a structure of smaller grains and relatively weaker preferred orientation compared to those obtained at higher substrate temperatures. At higher substrate temperatures, atoms have enough kinetic energy to diffuse to the preferred nucleation sites. Easy propagation of atoms results in the development of a strong preferred orientation. The crystallite size also has strong dependence on the substrate temperature.

From the diffractograms of Fig. 1 it is evident that the film texturing (preferred orientation) is strongly dependent on the substrate temperature. For example, while at 100 °C the (2 0 0) peak dominates, at 300 °C this peak decreases in favour of the (1 1 1) peak. For higher temperature, the (1 1 1) peak decreases again in favour of the (2 0 0) and (1 1 1) peaks. Texturing changes due to a different growth temperature is not an unusual phenomenon, as during the film growth a simultaneous film annealing is also taking place. This is in particular valid at higher temperatures. For example, we have observed in the past a texturing change for ZnO thin films: while for the as-deposited ZnO films, the (1 0 1) peak was the dominating peak, after annealing at 500 °C, the (0 0 2) peak dominated. Such results indicate that film orientation is self-optimized for each substrate temperature and that high temperatures favour the formation of nickel oxide films with larger crystalline size as shown [21,22].

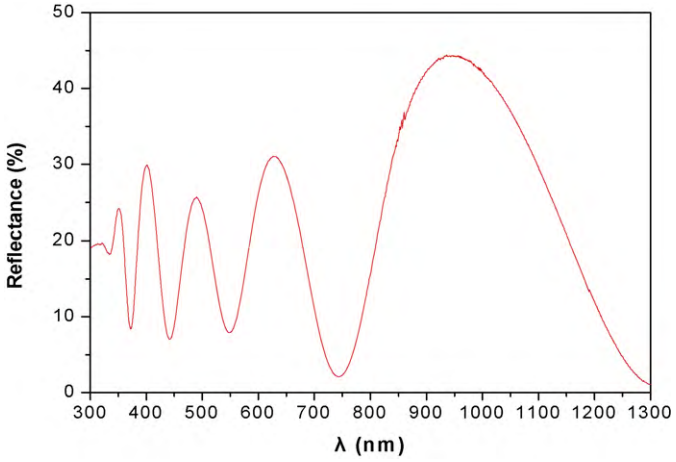

Fig. 2. Typical reflectivity spectrum of a NiO thin film.

3.2. Optical properties

The reflectance of the films was recorded in order to optically measure the film thickness. In Fig. 2, a typical reflectance spectrum can be seen. The Manifacier formula was used to calculate the thickness of the NiO thin films [23]:

$$t = \frac{M \cdot \lambda_1 \cdot \lambda_2}{2 \cdot [n(\lambda_1) \cdot \lambda_2 - n(\lambda_2) \cdot \lambda_1]} \quad (2)$$

where M is the number of oscillations between the two extremes ($M = 1$ between two consecutive maxima or minima), λ_1, $n(\lambda_1)$ and λ_2, $n(\lambda_2)$ are the corresponding wavelengths and indices of refraction.

The calculated thickness of the films is shown in Fig. 3. It is obvious that the thickness is affected by the substrate temperature mainly at low temperatures. The thickness is almost constant for temperature above 200 °C. The increase of the thickness is related to the increase of the grain size.

3.3. Electrical properties

The resistivity was measured by the Van der Pauw method (four point method) and its dependence on the substrate temperature is presented in Fig. 4. The resistivity is affected by the substrate

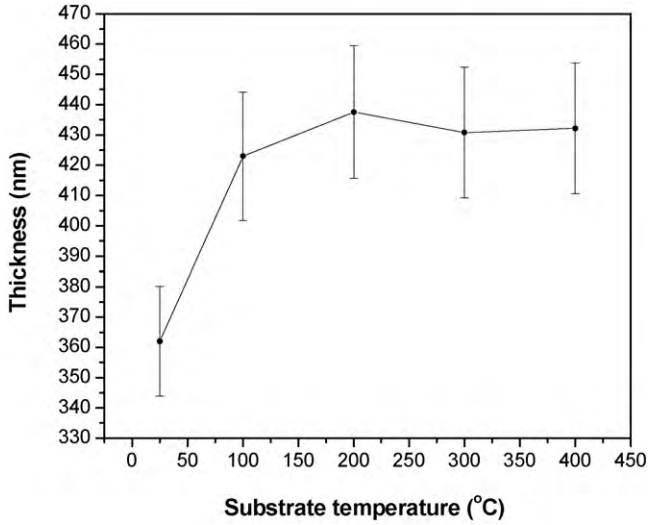

Fig. 3. Film thickness values at different deposition temperatures.

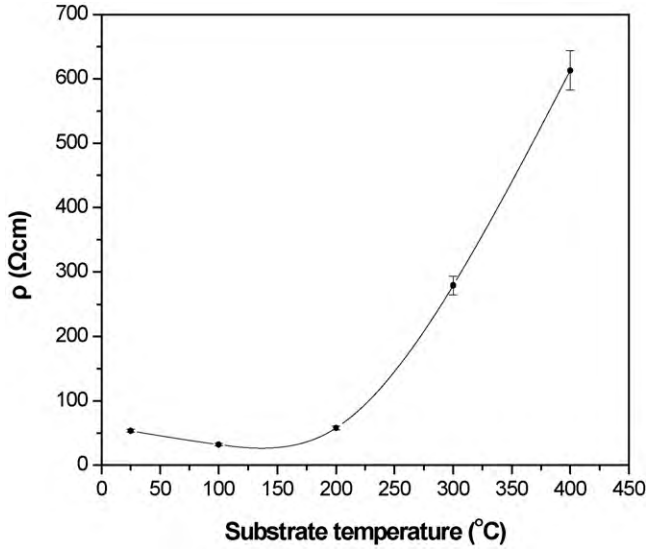

Fig. 4. Resistivity versus substrate temperature.

temperature, mainly at temperatures higher than 200 °C, and it increases with the substrate temperature.

The electrical conductivity of NiO is strongly related to the formation of microstructural defects inside the NiO crystallites, such as nickel vacancies and interstitial oxygen. As the XRD results indicate, the increasing substrate temperature leads to a more perfect crystalline structure thus decreasing the carrier concentration [20], which is induced by microstructure defects in the films. Non-stoichiometric nickel oxide is known as a p-type semiconductor, in which vacancies occur in cation sites. From each cation vacancy, two electron holes are formed. The carriers existing in NiO films are electron holes, which are responsible for the electrical conductivity of the undoped nickel oxide.

The resistivity (ρ) is inverse proportional to the product of the carrier concentration n_h with their mobility μ. The increase of the substrate temperature results in an increase of μ because the grain boundaries as well as the defects inside the crystallites become less, while the n_h reduces, due to the improved stoichiometry of the film. However, these two different approaches are responsible for the existence of the minimum of ρ (at approximately 150 °C). In the substrate temperature range between 25 and 150 °C, the decrease of the resistivity indicates that the increase of μ dominates the decrease of n_h. For substrate temperatures above 150 °C, the resistivity increase is attributed to the strong reduction of the carrier concentration n_h [20,22].

3.4. Nanomechanical properties

The load–displacement curves, to the same contact depth, for two representative NiO films, measured by nanoindentation are shown in Fig. 5. The load–displacement curves are used for the calculation of elasticity percentage by the formula:

$$\%R = \frac{A_{total} - A_1}{A_{total}} \times 100$$

where A_{total} is the total area under the load curve and A_1 is the area under the displacement curve. The dependence of $\%R$ on the substrate temperature is shown in Fig. 6.

It is clear that the area between the curves, which represents the plasticity percentage (1-$\%R$), is smaller as the substrate temperature rises. The film deposited without heating the substrate has the lowest elasticity percentage. For substrate temperatures >100 °C, the elasticity percentage increases due to narrower grain boundaries and thus better elastic behaviour.

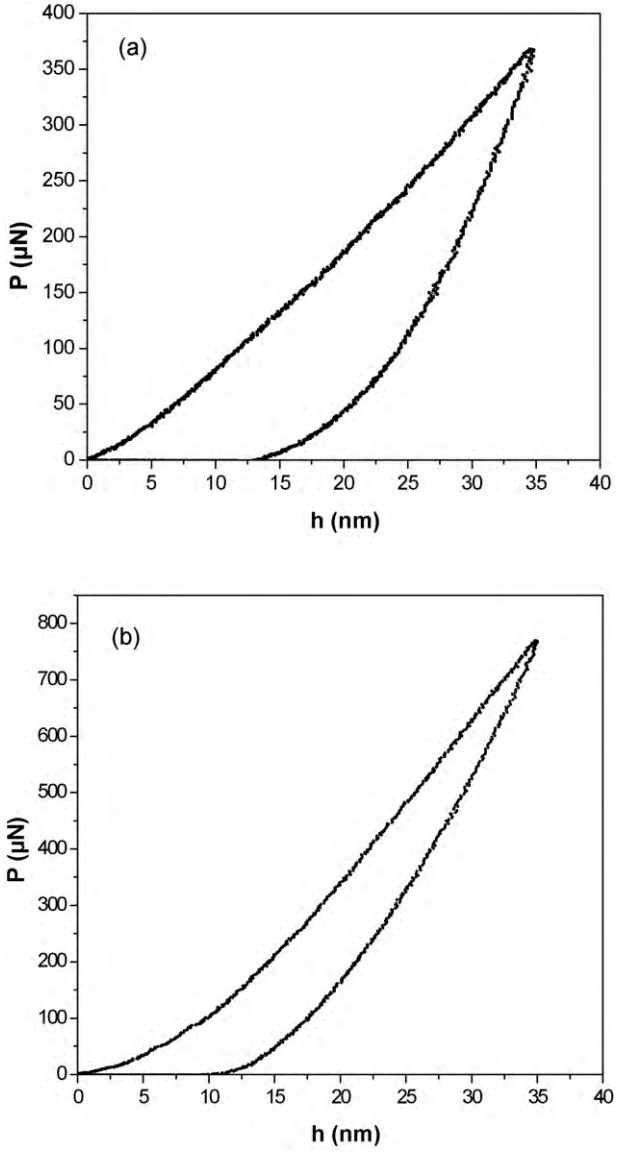

Fig. 5. Load–displacement curves from two representative NiO films. (a) NiO film deposited in room temperature (*RT*), and (b) NiO film deposited with substrate temperature 400 °C.

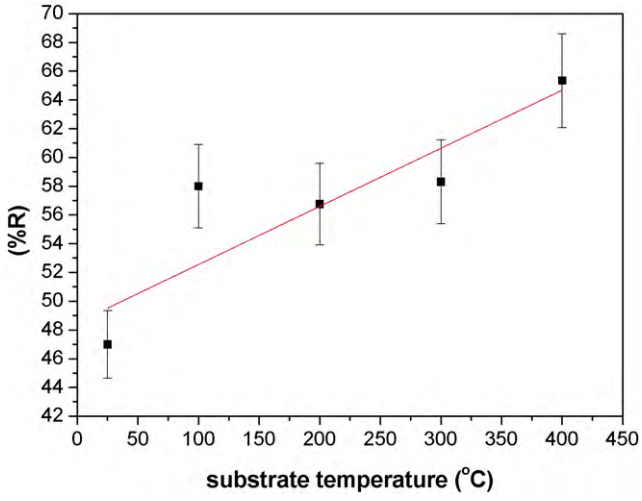

Fig. 6. Elasticity percentage %*R* versus substrate temperature.

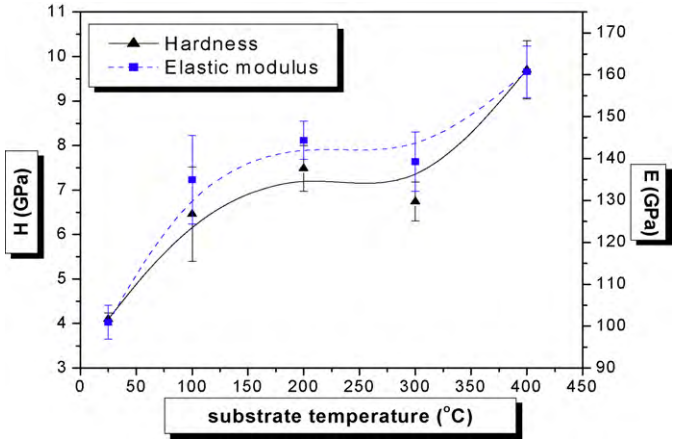

Fig. 7. Hardness (*H*) and elastic modulus (*E*) versus substrate temperature.

The hardness (*H*) and the elastic modulus (*E*) of NiO thin films are measured by nanoindentation and their dependence on the substrate temperature is presented in Fig. 7. It is obvious that the substrate temperature affects the hardness and the elastic modulus and its increase leads to an increase of these values.

We are not aware with any previous study concerning the measurement of *H* and *E* for NiO films. The *H* values measured in our work are in the range: 4.1–9.7 GPa, depending on the substrate temperature. Sputtered nickel films revealed hardness value of 3.12 GPa, while the hardness value of bulk nickel is 2.45 GPa [24]. Ni films fabricated by pulse electrodeposition revealed a hardness of about 7.8 GPa, and Young's modulus of about 215 GPa [25]. For Ni coatings prepared by powder injection laser cladding and for indentation depths, comparable with those of our work, hardness values ~9 GPa have been measured by nanoindentation [26]. Nanoindentation tests on electrodeposited Nickel specimens of nominal 20 nm grain size revealed a hardness value ~7 GPa. It should be noted that the strain-rate sensitivity is a strong function of grain size [27].

The *E* values measured in our work are in the range: 101–161 GPa, depending on the substrate temperature. Elastic modulus values for ternary Ni-base superalloy have been found in the range between 142 and 158 GPa [28].

In the case of titanium oxide films grown by using cathodic vacuum arc deposition [29], the nanohardness values are 6.9, 9.2 and 10.1 GPa for the as-deposited amorphous, post-annealed anatase and in situ heated anatase states respectively, depending on the O/Ti ratio. In other cases, the nanohardness was not dependent on the O/metal ratio. The nanohardness was constant over the O/Al range between 1.30 and 1.72 [30]. Hardness is a complex property related to the microstructure of the film and to the strength of interatomic forces, and depends on more than one variable [16].

Adhesion characteristics of the various coatings are examined using the nanoindenter under the applied loads (up to 1000 μN). Arai et al. [31] examined the failure modes of thin coatings following their indentation and argued that their adhesion characteristics could be categorized into five general groups depending on the presence (or not) and appearance of the radial or lateral cracks around the indentation. Based on the indentation traces in this work, only failure mode characterized by plastic deformation was occurred. The lack of cracking or flaking in this failure mode indicates that the coating has excellent adhesion properties.

The surface roughness of NiO thin films versus the substrate temperature is presented in Fig. 8. The increase of substrate temperature results in the decrease of the surface roughness. The roughness of the films deposited at *RT* is 25%, at 100 °C is 7%, at 200 °C is 27% and at 300 °C is 4% higher than the average grain size, respectively. On the other hand, the roughness of the film deposited at

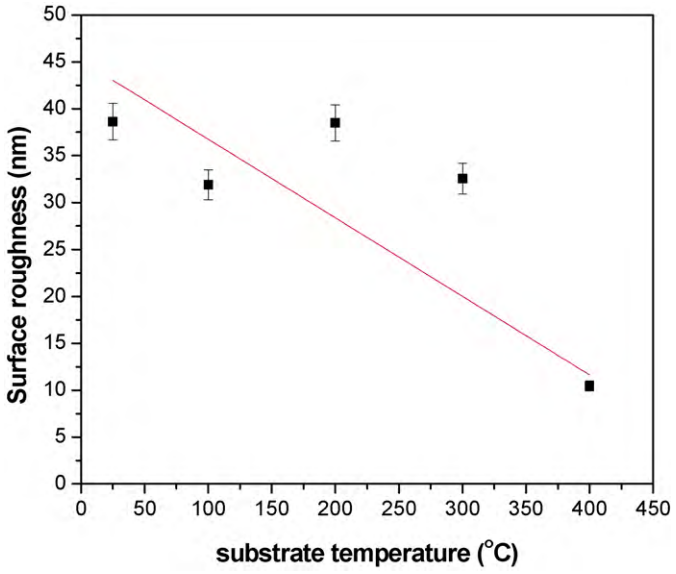

Fig. 8. Surface roughness of NiO films at different substrate temperatures.

400 °C is 66% lower than the average grain size. The roughness of the film deposited at RT is 40 nm and decreases to 10 nm when the substrate is heated at 400 °C during deposition. As a result, the surface of the films becomes smoother as the substrate temperature rises.

The deposited atoms on the substrate at low temperatures have the tendency to crystallize at planes with the lower energy creating rough surfaces. The decrease of the roughness occurs because the increase of the temperature offers enough thermal energy at atoms deposited on the substrate in order to crystallize at planes with lower roughness [32]. Chen et al. studied the effect of substrate temperature and the power on the roughness of NiO thin films. They also found that the sputtering power is an important deposition parameter that affects the surface roughness. In our case, the decrease of roughness is possible to happen by decreasing the laser fluence. Lower laser fluence will also lead to lower resistivity.

The surface roughness decreases with the temperature and the grain size substantially increases. This is very reasonable since the growth kinetics becomes more significant with increasing temperature. The observed behavior is consistent to the structural zone model (SZM) [33], which is valid for ZnO [34]. Thus, with increasing temperature we can observe a smooth and gradual transition from a fibrous microstructure (zone I), which is characterized by small grain size, low density and high surface roughness, to a more compact structure (zone II), which is characterized by bigger grain size, high density (close to bulk) and smooth surfaces. Taking into account that for a single phase material the hardness is correlated with density [35] then our data are consistent with this scenario, i.e. we observe a transition from small grain size/low density (hardness)/high roughness to bigger grain size/higher density (hardness)/lower roughness with increasing temperature. Such behaviour has been also observed for TiN films [36] and ZrO_2 [37].

The substrate temperature is therefore an important deposition parameter which affects the structural, electrical and nanomechanical properties of NiO thin films.

4. Conclusions

It was proved that the structural properties of NiO thin films were strongly affected by the substrate temperature. Improvement of crystalline structure implied bigger crystallite size. Furthermore, at higher substrate temperatures the film thickness remained almost constant. Bigger grain size resulted in less grain boundaries and this effect influenced the electrical properties, a fact that makes NiO thin films appropriate for microelectronics applications. Calculation of resistivity showed that it increased with the increase of substrate temperature. For the first time, the nanomechanical properties were studied and found that they were affected by the formation and improvement of crystalline structure. Nanoindentation testing of NiO thin films revealed an increase of hardness (H) and elastic modulus (E) and a decrease of surface roughness when increasing the substrate temperature.

Acknowledgements

This work has been partially supported by the "Nano-structured organic–inorganic hybrid materials—synthesis, diagnostics and properties" program no. 2005ΣE01330081 of TPCI/NHRF as a "Centre of Excellence", 2005.

References

[1] E. Fujii, A. Tomozawa, H. Torii, R. Takayama, Japanese Journal of Applied Physics 35 (1996) L328.
[2] H. Sato, T. Minami, S. Takata, T. Yamada, Thin Solid Films 236 (1993) 27.
[3] B. Sasi, K.G. Gopchandran, P.K. Manoj, P. Koshy, P. Prabhakara Rao, V.K. Vaidyan, Vacuum 68 (2003) 149.
[4] A.K. Roslik, V.N. Konev, A.M. Maltsev, Oxidation of Metals 43 (1995) 1.
[5] K.S. Ahn, Y.C. Nah, Y.E. Sung, Applied Surface Science 199 (2002) 259.
[6] X. Chen, N.J. Wu, L. Smith, A. Ignatiev, Applied Physical Letters 84 (2004) 2700.
[7] I. Fasaki, A. Giannoudakos, M. Stamataki, M. Kompitsas, E. György, I.N. Mihailescu, F. Roubani-Kalantzopoulou, A. Lagoyannis, S. Harissopulos, Applied Physics A 91 (2008) 487.
[8] A.M. Huntz, M. Andrieux, R. Molins, Materials Science and Engineering A 417 (2006) 8.
[9] Y. Wang, C. Ma, X. Sun, H. Li, Microporous Mesoporous Materials 71 (2004) 99.
[10] Z. Jiao, M. Wu, Z. Qin, H. Xu, Nanotechnology 14 (2003) 458.
[11] T.G. Souza Cruz, M.U. Hleinke, A. Gorenstein, Applied Physics Letters 81 (2002) 4922.
[12] M. Lee, S. Seo, D. Seo, E. Jeong, I.K. Yoo, Integrated Ferroelectrics 68 (2004) 19.
[13] L. Zbroniec, T. Sasaki, N. Koshizaki, Journal of Ceramic Processing Research 6 (2005) 134.
[14] B. Sasi, K.G. Gopchandran, Nanotechnology 18 (2007) 115613.
[15] M. Stamataki, D. Tsamakis, N. Brilis, I. Fasaki, A. Giannoudakos, M. Kompitsas, Physica Status Solidi A-Applied Research 205 (2008) 2064–2068.
[16] C.A. Charitidis, International Journal of Refractory Metals & Hard Materials 28 (2010) 51.
[17] S. Logothetidis, C. Charitidis, Thin Solid Films 353 (1999) 208.
[18] G. Carturan, G. Cocco, S. Enzo, R. Ganzerla, M. Lenarda, Materials Letters 7 (1988) 47.
[19] G. Pilstrom, Acta Chemica Scandinavica 15 (1961) 893.
[20] Y.M. Lu, W.S. Hwang, J.S. Yang, Surface & Coatings Technology 155 (2002) 231.
[21] Y.M. Lu, W.S. Hwang, J.S. Yang, H.C. Chuang, Thin Solid Films 420–421 (2002) 54.
[22] Z. Xuping, C. Guoping, Thin Solid Films 298 (1997) 53.
[23] J.C. Manifacier, J. Gasiot, J.P. Fillard, Journal of Physics E: Scientific Instruments 9 (1976) 1002.
[24] H.C. Barshilia, K.S. Rajam, Journal of Surface and Coatings Technology 155 (2002) 195.
[25] Y.F. Shen, W.Y. Xue, Y.D. Wang, Z.Y. Liu, L. Zuo, Journal of Surface & Coatings Technology 202 (2008) 5140.
[26] S. Graça, R. Colaço, R. Vilar, Journal of Surface & Coatings Technology 202 (2007) 538.
[27] R. Schwaiger, B. Moser, M. Dao, N. Chollacoop, S. Suresh, Journal of Acta Materialia 51 (2003) 5159.
[28] T. Schöberl, H.S. Gupta, P. Fratz, Journal of Materials Science and Engineering A 363 (2003) 211.
[29] H. Takikawa, T. Matsui, T. Sakakibara, A. Bendavid, P.J. Martin, Journal of Thin Solid Films 348 (1999) 145.
[30] K. Koski, J. Holsa, P. Juliet, Journal of Surface and Coatings Technology 116–119 (1999) 716.
[31] T. Arai, H. Fujita, M. Watanabe, Journal of Thin Solid Films 154 (1987) 387.
[32] H.-L. Chen, Y.-M. Lu, W.-S. Hwang, Journal of Surface and Coatings Technology 198 (2005) 138.
[33] J.A. Thornton, Annual Review in Material Science 7 (1977) 239.
[34] T. Schuler, T. Krajewski, I. Grobelsek, M.A. Aegerter, Thin Solid Films 502 (2006) 67.
[35] P. Patsalas, C. Charitidis, S. Logothetidis, Surface and Coatings Technology 125 (2000) 335.
[36] P. Patsalas, C. Gravalidis, S. Logothetidis, Journal of Applied Physics 96 (2004) 6234.
[37] K. Koski, J. Holsa, P. Juliet, Surface and Coatings Technology 120–121 (1999) 303.